

REPORT DOCUMENTATION PAGE

Form Approved
OMB No. 0704-0188

Public reporting burden for this collection of information is estimated to average 1 hour per response, including the time for reviewing instructions, searching existing data sources, gathering and maintaining the data needed, and completing and reviewing this collection of information. Send comments regarding this burden estimate or any other aspect of this collection of information, including suggestions for reducing this burden to Department of Defense, Washington Headquarters Services, Directorate for Information Operations and Reports (0704-0188), 1215 Jefferson Davis Highway, Suite 1204, Arlington, VA 22202-4302. Respondents should be aware that notwithstanding any other provision of law, no person shall be subject to any penalty for failing to comply with a collection of information if it does not display a currently valid OMB control number. **PLEASE DO NOT RETURN YOUR FORM TO THE ABOVE ADDRESS.**

1. REPORT DATE (DD-MM-YYYY) 30-07-2007		2. REPORT TYPE Technical Paper & Briefing Charts		3. DATES COVERED (From - To)	
4. TITLE AND SUBTITLE Aluminum Combustion in Solid Rocket Motor Chamber Environment (Preprint)				5a. CONTRACT NUMBER FA9300-05-C-0011	
				5b. GRANT NUMBER	
				5c. PROGRAM ELEMENT NUMBER	
6. AUTHOR(S) Merrill K. King (Software and Engineering Associates, Inc.)				5d. PROJECT NUMBER 492204JJ	
				5e. TASK NUMBER	
				5f. WORK UNIT NUMBER	
7. PERFORMING ORGANIZATION NAME(S) AND ADDRESS(ES) Software and Engineering Associates, Inc. 1802 N. Carson Street, Suite 200 Carson City NV 89701				8. PERFORMING ORGANIZATION REPORT NUMBER AFRL-PR-ED-TP-2007-375	
9. SPONSORING / MONITORING AGENCY NAME(S) AND ADDRESS(ES) Air Force Research Laboratory (AFMC) AFRL/PRS 5 Pollux Drive Edwards AFB CA 93524-70448				10. SPONSOR/MONITOR'S ACRONYM(S)	
				11. SPONSOR/MONITOR'S NUMBER(S) AFRL-PR-ED-TP-2007-375	
12. DISTRIBUTION / AVAILABILITY STATEMENT Approved for public release; distribution unlimited (PA #07380A).					
13. SUPPLEMENTARY NOTES For presentation at the 32 nd International Symposium on Combustion, McGill University, Montreal, Canada, 3-8 August 2008.					
14. ABSTRACT A model for prediction of particle radius and oxide cap size/shape versus time for an aluminum particle tracking a stream-tube through a solid rocket motor port has been developed. Following preliminary calculations leading to a postulated flame structure, a quasi-steady model to predict instantaneous consumption of aluminum and generation of condensed oxide (both as a cap on the aluminum particle and as smoke) as a function of instantaneous particle size, ambient conditions, and cumulative amount of oxide in the cap was developed. Finally, this model was imbedded into a framework tracking evolution of particle size, oxide cap size, and ambient conditions, which change as the particle travels along a stream-tube consuming oxidizer and releasing heat. Qualitative agreement was found between predictions and limited observations.					
15. SUBJECT TERMS					
16. SECURITY CLASSIFICATION OF:			17. LIMITATION OF ABSTRACT	18. NUMBER OF PAGES	19a. NAME OF RESPONSIBLE PERSON
a. REPORT	b. ABSTRACT	c. THIS PAGE			Hieu Nguyen
Unclassified	Unclassified	Unclassified	SAR	42	19b. TELEPHONE NUMBER (include area code) N/A

Aluminum Combustion in a Solid Rocket Motor Environment

Merrill K. King
Consultant
Software and Engineering Associates, Inc.
Carson City, NV 89701
USA

FAX: 202-358-3091
E-Mail: mking9524@verizon.net

6. Heterogeneous Combustion

Main Body Text:	2973 words
8 Figures:	1600 words
Equations:	900 words
References:	70 words
Total:	5543 words

Distribution A: Public Release; distribution unlimited

ABSTRACT

A model for prediction of particle radius and oxide cap size/shape versus time for an aluminum particle tracking a stream-tube through a solid rocket motor port has been developed. Following preliminary calculations leading to a postulated flame structure, a quasi-steady model to predict instantaneous consumption of aluminum and generation of condensed oxide (both as a cap on the aluminum particle and as smoke) as a function of instantaneous particle size, ambient conditions, and cumulative amount of oxide in the cap was developed. Finally, this model was imbedded into a framework tracking evolution of particle size, oxide cap size, and ambient conditions, which change as the particle travels along a stream-tube consuming oxidizer and releasing heat. Qualitative agreement was found between predictions and limited observations.

ABSTRACT

A model for prediction of particle radius and oxide cap size/shape versus time for an aluminum particle tracking a stream-tube through a solid rocket motor port has been developed. Following preliminary calculations leading to a postulated flame structure, a quasi-steady model to predict instantaneous consumption of aluminum and generation of condensed oxide (both as a cap on the aluminum particle and as smoke) as a function of instantaneous particle size, ambient conditions, and cumulative amount of oxide in the cap was developed. Finally, this model was imbedded into a framework tracking evolution of particle size, oxide cap size, and ambient conditions, which change as the particle travels along a stream-tube consuming oxidizer and releasing heat. Qualitative agreement was found between predictions and limited observations.

BACKGROUND/PRELIMINARY CALCULATIONS

In 1995, Brooks and Beckstead [1] published a paper in which the state-of-the-art regarding aluminum particle combustion modeling and data was well reviewed. Subsequent papers by Babuk [2], DesJardin [3], Fabignon [4], and Bazyn [5] added further information in this area. Due to word limitations, these papers will not be discussed in detail. The model development presented in the next section drew on all of these papers as well as on the following preliminary calculations.

(1) Aluminum partial pressure adjacent to the particle surface was determined as a function of surface temperature from $K_P = P_{Al,g} \text{ (atm)} = \exp(-\Delta G^0/RT_s)$ where ΔG^0 is the change in free energy accompanying vaporization as tabulated in the JANAF Thermochemical Tables [6].

(2) This relationship was combined with a simplified B-Number analysis (as described in Turns' textbook [7]) to estimate the surface temperature: this calculation indicates that the surface temperature is far below the boiling point of aluminum at normal motor operating pressures, counter to assumptions made in some previous models.

(3) From several sets of thermochemistry calculations, it was concluded that the predominant Al_xO_y specie would be Al_2O_3 liquid at any place in the flame structure where the oxygen/aluminum atomic ratio is high enough to take it there.

(4) Further free energy calculations indicated that Babuk's [2] claim that $4Al(l) + Al_2O_3(l)$ will convert to $3Al_2O(g)$ at the oxide-aluminum interface in the oxide cap region is unlikely.

(5) Additional thermochemistry calculations indicated that likely reactions at the aluminum surface are Al vaporization and $4\text{AlO} \rightarrow \text{Al}_2\text{O}_3(\text{l}) + \text{Al}_2\text{O}(\text{g})$.

(6) Still more thermochemistry calculations indicate that if the principal oxidizers are CO_2 and H_2O (typical in an aluminized solid rocket motor) the likely reaction sequence is $\text{Al}(\text{g}) + \text{CO}_2 \rightarrow \text{AlO}/1/2\text{Al}_2\text{O}_2 + \text{CO}$ and $\text{Al}(\text{g}) + \text{H}_2\text{O} \rightarrow \text{AlO}/1/2\text{Al}_2\text{O}_2 + \text{H}_2$ at a primary flame sheet followed by further oxidation to $\text{Al}_2\text{O}_3(\text{l}) + \text{CO} + \text{H}_2$ at an outer condensation sheet.

(7) Finally, thermochemistry calculations were used to estimate the fraction of Al_xO_x which will appear as monomer rather than dimer as a function of flame sheet temperature: these calculations yielded Mass Fraction Monomer = $0.122 + 0.000577(T-3500)$

MODEL DEVELOPMENT

A sketch of the postulated quasi-steady combustion model is presented as Figure 1. (As will be discussed later, this model is imbedded in another code in which the progressions of boundary conditions as the particle travels along a given stream-tube are updated.) As shown, the structure is composed of three zones (Inner, Middle, and Outer) bounded by the droplet surface, an infinitesimally thin flame sheet where primary oxidation occurs, and another infinitesimally thin zone where final oxidation to Al_2O_3 and oxide condensation occur. It is postulated that, in addition to vaporization of aluminum from the particle surface, AlO diffusing back to the surface from the primary flame sheet undergoes collision-limited reaction with the surface to form Al_2O_3 liquid, which is added to the cap, and $\text{Al}_2\text{O}(\text{g})$ (via $4\text{AlO} \rightarrow \text{Al}_2\text{O}_3(\text{l}) + \text{Al}_2\text{O}(\text{g})$), with the aluminum vapor and Al_2O then traveling outward toward the primary flame sheet. At this flame sheet, it is assumed that the aluminum vapor reacts instantaneously with CO_2 and H_2O (coming from the outer regions) to form a mixture of AlO and Al_2O_2 , with the ratio of monomer to dimer being determined by the flame zone temperature, as discussed earlier. Based on the preliminary calculations, it is assumed that the Al_2O does not react here but instead travels outward along with the AlO/ Al_2O_2 mixture to the condensation sheet where the suboxides react with additional carbon dioxide and water vapor to produce $\text{Al}_2\text{O}_3(\text{l})$, hydrogen, and carbon monoxide. It is further assumed (flame sheet approximation) that there are no gas phase reactions occurring in the three zones permitting standard development of algebraic equations describing the transport of species and enthalpy across the three zones. Fick's first law, with "effective" binary diffusion coefficients calculated at the midpoint temperature of each zone and with Lewis Number = 1 is used in development of these equations.

Total enthalpy (chemical plus sensible) is assumed to be constant across each zone (no reactions) with the values of the total enthalpy in each zone being determined by energy balances at the surface, at the primary flame sheet, and at the condensation sheet, accounting for source/sink terms associated with reactions at those locations. In addition, the outer boundary conditions, which would normally be specified at an infinite radius, are instead applied at a radius specified by the spacing of the particles relative to one another in the stream-tube flow. An “inert” specie, representing all the free-stream species other than CO₂, H₂O, CO, and Al is included as part of the overall gas composition. Obviously, for a quasi-steady analysis (no accumulation terms) its flux through each zone will be zero, as will fluxes of CO and H₂O in the inner zone, where diffusion and convection of these species are required to cancel out. The aluminum oxide smoke produced at the condensation zone as a ‘sink’ term is assumed to disappear from the system though its thermal effects must be included. For solution of this problem, the condensation temperature has to be a model input, based on the previously discussed thermochemistry considerations.

Boundary conditions for solution of these equations describing the aluminum burning rate, deposition of oxide at the surface (as characterized by oxide cap size) and production of oxide smoke at the condensation “sink” region are brought into the single particle analysis from the wrap-around code in which this analysis is imbedded. These conditions include free-stream temperature (T_{AMB}), free-stream mass fractions of CO₂, H₂O, CO, Al, and “inert” ($Y_{j,AMB}$), instantaneous particle radius (r_{surf}), fraction of surface coated by oxide (b), pressure (P), amount of aluminum still unburned (M_{Al}), and mass of oxide accumulated in the cap (M_{OX}).

In line with the assumption of infinitesimally thin reaction/condensation sheets, it is assumed that the mass fractions of Al(g), H₂O, and CO₂ at the flame sheet are zero as are the mass fractions of Al₂O and Al_xO_x at the condensation sheet. In addition, the ratio of AlO to Al₂O₂ is assumed to be frozen at the flame sheet radius value elsewhere. The remaining unknowns after application of these assumptions/approximations are mass fractions of species and mass fluxes through the three zones

$$\text{At } r = r_{surf} : Y_{Al,S}, Y_{Al_xO_x,S}, Y_{CO,S}, Y_{H_2,S}, Y_{INERT,S}$$

$$\text{At } r = r_{FZ} : Y_{AlO,FZ}, Y_{Al_2O_2,FZ}, Y_{Al_2O,FZ}, Y_{CO,FZ}, Y_{H_2,FZ}, Y_{INERT,FZ}$$

$$\text{At } r = r_{CZ} : Y_{H_2,CZ}, Y_{CO,CZ}, Y_{CO_2,CZ}, Y_{H_2O,CZ}, Y_{INERT,CZ}$$

Inner Zone ($r_s < r < r_{FZ}$) :

$$\dot{m}_{Al,Inner}, \dot{m}_{Al_xO_x,Inner}, \dot{m}_{Al_2O,Inner}, \dot{m}_{Net,Inner}$$

Mid Zone ($r_{FZ} < r < r_{CZ}$)

$$\dot{m}_{Al_2O, Mid}^{\dot{Y}}, \dot{m}_{Al_xO_x, Mid}^{\dot{Y}}, \dot{m}_{H_2, Mid}^{\dot{Y}}, \dot{m}_{H_2O, Mid}^{\dot{Y}}, \dot{m}_{CO, Mid}^{\dot{Y}}, \dot{m}_{CO_2, Mid}^{\dot{Y}}, \dot{m}_{Net, Mid}^{\dot{Y}}$$

Outer Zone ($r_{CZ} < r < r_{AMB}$) :

$$\dot{m}_{H_2, Outer}^{\dot{Y}}, \dot{m}_{H_2O, Outer}^{\dot{Y}}, \dot{m}_{CO, Outer}^{\dot{Y}}, \dot{m}_{CO_2, Outer}^{\dot{Y}}, \dot{m}_{Net, Outer}^{\dot{Y}}$$

Additional unknowns are the surface and flame-sheet temperatures (T_{Surf} , T_{FZ}), total enthalpy flux across each zone (H_{INNER} , H_{MID} , and H_{OUT}), flame sheet radius (r_{FZ}), Condensation Sheet Radius (r_{CZ}), mass rate of aluminum consumption at the surface (dM_{AL}/dt), mass rate of oxide deposition at the surface (dM_{OX}/dt) and the mass rate of production of oxide smoke at the condensation radius (m_{SINK}), for a total of 42 unknowns.

Accordingly, 42 equations are required for closure of the problem, given the boundary conditions brought in at each instant of time from the wrap-around stream-tracking code. Four equations are provided by integration of the convective/diffusive species flux equations (in the absence of reaction) across the outer zone:

$$\frac{\dot{m}_{net, outer}^{\dot{Y}}}{4\pi\rho D(1-\beta)} \left(1/r_{CZ} - 1/r_{AMB}\right) = \ln \frac{\dot{m}_{net, outer}^{\dot{Y}} Y_{j, AMB} - \dot{m}_{j, Outer}^{\dot{Y}}}{\dot{m}_{net, outer}^{\dot{Y}} Y_{j, CZ} - \dot{m}_{j, outer}^{\dot{Y}}} \quad (1-4)$$

$$j = CO, CO_2, H_2, H_2O$$

Similarly, six additional equations are provided by integration of the convective/diffusive transport equations across the middle zone:

$$\frac{\dot{m}_{net, Mid}^{\dot{Y}}}{4\pi\rho D(1-\beta)} \left(1/r_{FZ} - 1/r_{CZ}\right) = \ln \frac{\dot{m}_{net, Mid}^{\dot{Y}} Y_{j, CZ} - \dot{m}_{j, Mid}^{\dot{Y}}}{\dot{m}_{net, Mid}^{\dot{Y}} Y_{j, FZ} - \dot{m}_{j, Mid}^{\dot{Y}}} \quad (5-10)$$

$$j = CO, CO_2, H_2, H_2O, Al_xO_x, Al_2O$$

Five more equations are produced through integration of the convective/diffusive transport equations across the inner zone:

$$\frac{\dot{m}_{net, Inner}^{\dot{Y}}}{4\pi\rho D(1-\beta)} \left(1/r_{Surf} - 1/r_{FZ}\right) = \ln \frac{\dot{m}_{net, Inner}^{\dot{Y}} Y_{j, FZ} - \dot{m}_{j, Inner}^{\dot{Y}}}{\dot{m}_{net, Inner}^{\dot{Y}} Y_{j, Surf} - \dot{m}_{j, Inner}^{\dot{Y}}} \quad (11-15)$$

$$j = CO, H_2, Al_xO_x, Al_2O, Al$$

where:

$$\dot{m}_{net}^{\dot{Y}} = \sum \dot{m}_j^{\dot{Y}} \quad \text{for each zone} \quad (16-18)$$

In addition, Y_{Inert} at the surface, flame sheet, and condensation sheet are obtained from:

$$\sum Y_j = 1.0 \quad \text{for each location} \quad (19-21)$$

Integration of differential equations for total (chemical plus sensible) enthalpy across each of the three zones (Inner, Middle, and Outer yields three equations relating temperatures at $r = r_{Surf}$, $r = r_{FZ}$, and $r = r_{CZ}$ to the enthalpy fluxes in each zone ($H_{F,Inner}$, $H_{F,MID}$, and $H_{F,Outer}$) of the form:

$$\frac{\sum \dot{m}_{j,Outer}^{\dot{Y}} c_{p,j}}{4\pi\rho D(1-\beta)\bar{c}_p} (1/r_{CZ} - 1/r_{Amb}) = \ln \frac{(\sum \dot{m}_{j,Outer}^{\dot{Y}} c_{p,j})T_{Amb} + \sum \dot{m}_j^{\dot{Y}} a_j - H_{F,Outer}}{(\sum \dot{m}_{j,Outer}^{\dot{Y}} c_{p,j})T_{CZ} + \sum \dot{m}_j^{\dot{Y}} a_j - H_{F,Outer}} \quad (22)$$

$$\frac{\sum \dot{m}_{j,Mid}^{\dot{Y}} c_{p,j}}{4\pi\rho D(1-\beta)\bar{c}_p} (1/r_{FZ} - 1/r_{CZ}) = \ln \frac{(\sum \dot{m}_{j,Mid}^{\dot{Y}} c_{p,j})T_{CZ} + \sum \dot{m}_j^{\dot{Y}} a_j - H_{F,Mid}}{(\sum \dot{m}_{j,Mid}^{\dot{Y}} c_{p,j})T_{FZ} + \sum \dot{m}_j^{\dot{Y}} a_j - H_{F,Mid}} \quad (23)$$

$$\frac{\sum \dot{m}_{j,Inner}^{\dot{Y}} c_{p,j}}{4\pi\rho D(1-\beta)\bar{c}_p} (1/r_{Surf} - 1/r_{FZ}) = \ln \frac{(\sum \dot{m}_{j,Inner}^{\dot{Y}} c_{p,j})T_{FZ} + \sum \dot{m}_j^{\dot{Y}} a_j - H_{F,Inner}}{(\sum \dot{m}_{j,Inner}^{\dot{Y}} c_{p,j})T_{Surf} + \sum \dot{m}_j^{\dot{Y}} a_j - H_{F,Inner}} \quad (24)$$

where the a_j 's are $(h^0 - c_p T^0)_j$ values obtained from curve fits for each species and the H_F 's are obtained from enthalpy balances at the surface, flame sheet, and condensation sheet as:

$$H_{F,Inner} = 0.593 \dot{m}_{Al_2O_3,Inner}^{\dot{Y}} h_{Al_2O_3(l),T_{Surf}} + \dot{m}_{Al,Inner}^{\dot{Y}} h_{Al(l),T_{Surf}} \quad (25)$$

$$H_{F,Mid} = H_{F,Inner} \quad (26)$$

$$H_{F,Outer} = H_{F,Mid} - \dot{m}_{Sink}^{\dot{Y}} h_{Al_2O_3(l),T_{CZ}} \quad (27)$$

Next, there are several stoichiometric relationships to be invoked:

$$\dot{n}_{CO_2,Outer} / 28.011 = -\dot{n}_{CO_2,Outer} / 44.011 \quad (28)$$

$$\dot{n}_{H_2O,Outer} / 2.016 = -\dot{n}_{H_2O,Outer} / 18.016 \quad (29)$$

$$(\dot{n}_{CO_2,Mid} - \dot{n}_{CO_2,Outer}) / 44.011 = (\dot{n}_{CO_2,Outer} - \dot{n}_{CO_2,Mid}) / 28.011 \quad (30)$$

$$(\dot{n}_{H_2O,Mid} - \dot{n}_{H_2O,Outer}) / 18.016 = (\dot{n}_{H_2O,Outer} - \dot{n}_{H_2O,Mid}) / 2.016 \quad (31)$$

$$\begin{aligned} \dot{n}_{Al_2O_3,Mid} / 86 + \dot{n}_{Al_2O_3,Mid} / 35 = & (\dot{n}_{CO_2,Mid} - \dot{n}_{CO_2,Outer}) / 44.011 \\ & + (\dot{n}_{H_2O,Mid} - \dot{n}_{H_2O,Outer}) / 18.016 \end{aligned} \quad (32)$$

$$\dot{n}_{Sink,CZ} = (102 / 70) \dot{n}_{Al_2O_3,Mid} + (102 / 86) \dot{n}_{Al_2O_3,Mid} \quad (33)$$

$$\dot{n}_{Al_2O_3,Inner} = -(70 / 102) \dot{n}_{Al_2O_3,Inner} \quad (34)$$

$$dM_{Al} / dt = -\dot{n}_{Al,Inner} \quad (35)$$

$$dM_{OX} / dt = (-102 / 172) \dot{n}_{AlO,Inner} \quad (36)$$

$$\dot{n}_{Al,Inner} / 27 = (\dot{n}_{Al_2O_3,Inner} - \dot{n}_{Al_2O_3,Inner}) / 43 \quad (37)$$

$$\dot{n}_{Al_2O_3,Inner} = \dot{n}_{Al_2O_3,Mid} \quad (38)$$

$$\dot{n}_{Al,Inner} / 27 = -\dot{n}_{CO_2,Mid} / 44 - \dot{n}_{H_2O,Mid} / 18 \quad (39)$$

Finally:

$$Y_{AlO,FZ} / (Y_{AlO,FZ} + Y_{Al_2O_3,FZ}) = 0.122 + 0.000577 (T_{FZ} - 3500.0) \quad (40)$$

$$-\dot{n}_{Al_2O_3,Inner} = v \frac{3653 r_{Surf}^2 P (1 - \beta) (Y_{AlO,Surf} / 43)}{\sqrt{T_{Surf}} (\sum Y_{j,Surf} / (MW_{j,Surf}))} \quad (41)$$

(from collision rate theory, with v being the input fraction of collisions of AlO at the surface resulting in reaction), and

$$P(Y_{Al,Surf} / 27) / (\sum Y_{j,s} / MW_j) = \exp(12.43 - 34680 / T_{Surf}) \quad (42)$$

OUTLINE OF SOLUTION PROCEDURE

First, values for the ambient temperature (values at $r = r_{AMB}$) and the ambient mass fractions of CO, CO₂, H₂, H₂O, and inert (all other species being lumped as inert, with straightforward calculation of an average molecular weight for that inert) were imported along with current particle radius (r_{Surf}), pressure (P), and fraction of the particle surface covered with oxide (b) from the stream-tube tracking wrap-around program described in the next section. Given these values, the approach taken to solving this set of equations consisted of a double-nested trial-and-error loop in which dM_{Al}/dt and dM_{OX}/dt were first guessed and used to sequentially calculate other parameters until Y_{CO_2} at the flame sheet was calculated. If this answer was not 0.0, the guess on dM_{Al}/dt was adjusted and this inner loop was repeated until the CO₂ mass fraction at the surface did equal zero. As part of this loop a value for the condensation radius was calculated. Next, the remaining equations were used to arrive at a second value for the condensation radius based on the enthalpy balances. If the two values of condensation radius did not agree, a new value of dM_{OX}/dt was chosen, the entire inner loop was reconverged, and another comparison of the condensation radius calculated in the inner loop with a new value calculated from the enthalpy balances was made. This overall procedure was continued until both loops were converged. During all of these loops, updates on surface temperature, flame sheet temperature, and midpoint temperature values for each zone were calculated and used to update values on the density-diffusivity products in each zone and the mean heat capacities in each zone. In addition, the average molecular weights of the gas mixtures in each zone were continuously updated. More details on this approach can be obtained from the author. Hard-wired values of the various $c_{p,j}$'s, a_j 's, and values of species enthalpies at a reference temperature were built into the computer code.

Only on the first call from the wrap-around stream-tube tracking code is this process somewhat time-consuming if bad initial guesses are made. On subsequent calls, made at small time intervals, the changes in ambient conditions, particle radius, and fraction coating of oxide are quite small and the final converged solution for the previous time step is most adequate for rapid convergence in the present time step.

WRAP-AROUND STREAM-TRACKING CODE

The model described above is imbedded in a stream-tracking code which keeps track of all of ambient and particle parameters as the particle travels through the rocket motor, heating (releasing heat) and eating (consuming oxidizer) as it goes. Inputs to this code include the initial particle size, initial oxide thickness, pressure, stagnant film radius (based on particle spacing), and several initial guesses for parameters being calculated in the imbedded code at zero time.

Included in the code are curve fits for ambient species mass fractions and ambient temperature as functions of the cumulative percentage of aluminum burned for the propellant formulation of interest. Curve fits for condensed aluminum and aluminum oxide densities as functions of temperature are also included. In addition, a rather simple geometry-based algorithm for the calculation of the fractional surface coating by the molten oxide cap as a function of the instantaneous masses of aluminum and oxide cap is included.

The densities of liquid aluminum and aluminum oxide are built in as:

$$\rho_{Al} \text{ (gm/cm}^3\text{)} = 2.364[1.0 - 0.00002268(T - 933)] \quad (43)$$

$$\rho_{Al_2O_3} \text{ (gm/cm}^3\text{)} = 2.998[1.0 - 0.00003731(T - 2327)] \quad (44)$$

where T is in degrees-Kelvin, and are used to relate the aluminum particle radius to the aluminum mass and the oxide cap volume to the cap oxide mass.

The geometry of the oxide cap, which leads to a relationship between the fractional aluminum surface area coverage and the volume (and thus mass) of oxide in the cap and volume (mass) of the aluminum sphere was calculated by assuming that the intersection of the Al and Al₂O₃ is represented by the intersection of two spheres at a 90-degree angle (probably somewhat of an oversimplification) as depicted in Figure 2. For a 90° intersection, it can be shown that the distance between the centers of the spheres (d) is related to the aluminum droplet radius (R) and the oxide lobe radius (r) by:

$$d = \sqrt{R^2 + r^2} \quad (45)$$

and that the intersection of the spheres is a circle with radius:

$$a = rR/\sqrt{R^2 + r^2} \quad (46)$$

It can also be shown that the volume common to both spheres is:

$$V = \pi(R + r - d)^2(d^2 + 2dr - 3r^2 + 2dR + 6rR - 3R^2)/12d \quad (47)$$

and that the volume of the oxide cap is:

$$VOLOX = (4/3)\pi r^3 - V \quad (48)$$

Since the cap radius (r) is not initially known, but VOLOX is known via the cumulative oxide cap mass accumulation, an iterative procedure is used to find a

cap radius for a given value of the aluminum sphere radius which gives the correct value for VOLOX. The linear angle α (see Figure 2) is then calculated as:

$$\alpha = \arcsin(a / R) \quad (49)$$

and the solid angle as:

$$SA = 2 \pi (1 - \cos \alpha) \quad (50)$$

The fraction of the aluminum sphere radius covered with oxide is finally calculated as:

$$\beta = SA / 4 \pi = (1 - \cos \alpha) / 2 \quad (51)$$

As mentioned earlier, as the aluminum particle burns, it releases heat and consumes oxidizer from its surroundings. To treat these changes in the ambient conditions, correlations of the various species mass fractions, temperature, and molecular weight of the "inert" were generated as functions of the cumulative percentage of aluminum burned, assuming no mixing with adjacent stream tubes or diffusion/conduction of species/heat along the stream tube. For the particular formulation of interest (70/18/12 AP/Al/HTPB), the following correlations (with X being the cumulative weight percent aluminum burned) were built into the code:

$$Y_{H_2} = 0.008 + 0.00022X \quad (52)$$

$$Y_{H_2O} = 0.270 - 0.00134X \quad (53)$$

$$Y_{CO} = 0.180 + 0.00160X \quad (54)$$

$$Y_{CO_2} = 0.174 - 0.002431X + 0.00001047X^2 \quad (55)$$

$$Y_{INERT} = 0.368 + 0.001951X - 0.00001047X^2 \quad (56)$$

$$MW_{INERT} = 33.28 - 0.0185 X - 0.000242 X^2 \quad (57)$$

$$T_{Amb} = 2550. + 10.687X - 0.03188X^2 \quad \text{for } X < 70$$

$$T_{Amb} = 3110. + 14.666(X - 70.) \quad \text{for } X > 70 \quad (58)$$

The overall operation of this code is outlined below:

- (1) Calculate initial mass of aluminum and oxide cap. Set Time = 0
- (2) Calculate initial oxide lobe radius and fraction of aluminum surface covered (β)
- (3) Calculate initial ambient temperature and composition.
- (4) Call aluminum combustion subroutine, getting back mass consumption rate of aluminum and generation rates of oxide cap and oxide smoke.
- (5) Take a small time step and calculate masses of aluminum burned and oxides generated over that step.
- (6) Calculate new value of aluminum mass and, from that and the initial mass, cumulative percentage burned.
- (7) Calculate new values of aluminum and oxide cap volumes
- (8) Using Equations 52-58, calculate new ambient condition values.
- (9) Using the geometric analysis outlined earlier, calculate a new value for fraction of the aluminum particle surface area blocked by the oxide cap.
- (10) Call the aluminum combustion subroutine again and continue with Steps 5-10 ad infinitum. Track cumulative amount of aluminum remaining, percent burned, cumulative oxide smoke production, and cumulative amount of oxide in the cap.

SAMPLE PROBLEM DEFINITION AND OUTPUT

The sample problem entails a 70/18/12 AP/Aluminum/HTPB formulation burning at 68 atmospheres, producing 100-micron radius aluminum particles with a one-micron thick initial oxide coating, which is assumed to immediately draw up into a lobe on one side of the particle. The input aluminum oxide condensation temperature was 4000K and the input reaction efficiency of $\text{AlO}/\text{Al}_2\text{O}_2$ gas molecules striking the virgin aluminum surface was unity. The input effective ambient radius around each particle was set based on the aluminum particle spacing in the flow through the rocket motor (for this case, approximately 10 times the initial particle radius.) Results are presented in Figures 3-8.

The percentage (mass) of the particle consumed is plotted against time from ignition out to approximately 120 milliseconds in Figure 3. The percent consumed increases monotonically with time, with a constantly decreasing slope

of the curve. Thus, approximately 55% of the mass has been consumed at 40 msec, 70% at 60 msec, 90% at 100 msec, and 98% at 120 msec (where the calculation was terminated).

In Figure 4, the aluminum particle radius and the radius of the oxide lobe are also plotted against time. The aluminum radius is seen to decrease (slightly less than linearly) with time, while the oxide cap radius increases monotonically with time, rapidly at first but at a decreasing rate with increasing time. Beyond approximately 60 msec, the oxide cap lobe radius is larger than the aluminum particle radius.

Since in classical diffusion-limited droplet combustion, a d^2 -law applies, with droplet radius squared decreasing linearly with time, the square of the predicted particle radius was plotted against time in Figure 5. A significant deviation from d -squared behavior is observed with the absolute value of the slope of the curve decreasing significantly with time. This behavior is largely a result of the fact that the fraction of the aluminum surface blocked by the oxide cap increases with time as shown in Figure 6.

As discussed earlier, part of the aluminum oxide appears in the form of smoke at the condensation zone, while part deposits on an accumulating cap at the aluminum particle surface. The split is, of course of interest due to the very different hydrodynamic behaviors of the two fractions. Accordingly fraction of the oxide appearing in the cap is plotted against time in Fig. 7—this is seen to asymptote to about 20 percent. Finally, in Figure 7, sketches of the geometries of the aluminum and the oxide cap are presented on a common scale: as may be seen, the final oxide cap radius is predicted to be approximately 70% of the original aluminum particle radius.

Acknowledgement: Support for this effort from SEA and the US Air Force via Contract FA-9300-05-C-0011 is gratefully acknowledged

REFERENCES

1. Brooks, K. P., and Beckstead. M. W., JPP, 11, 4, July-Aug, 1995.
2. Babuk, V. A., and Vasilyev, V. A., JPP, 18, 4, July-Aug, 2002.
3. DesJardin, P. E., Felske, J. D., and Carrara, M. D., JPP, 21, 3, May-June, 2005.
4. Fabignon, Y., Orlandi, O., Trubert, J. F., Lambert, D., and Dupays, J., AIAA Paper 2003-4807, July, 2003.
5. Bazyn, T., Krier, H., and Glumac, N., JPP, 21, 4, July-Aug, 2005.
6. Chase, M., NIST-JANAF Thermochemical Tables, 4th Ed., Monograph #9, 1998.
7. Turns, S. R., An Introduction to Combustion, 2nd Edition, 2000.

FIGURE CAPTIONS

Figure 1. Sketch of Aluminum Combustion Model

Figure 2. Sketch of Postulated Al-Al₂O₃ Lobe Geometry

Figure 3. Percentage Aluminum Burned Versus Time

Figure 4. Radius of Al Sphere and Oxide Cap Lobe Versus Time

Figure 5. Square of Radius of Aluminum Sphere Versus Time

Figure 6. Fraction of Al Surface Area Blocked By Oxide Cap Versus Time

Figure 7. Percentage of Oxide product Appearing in Cap Versus Time

Figure 8. Evolution of Al-Al₂O₃ Shapes

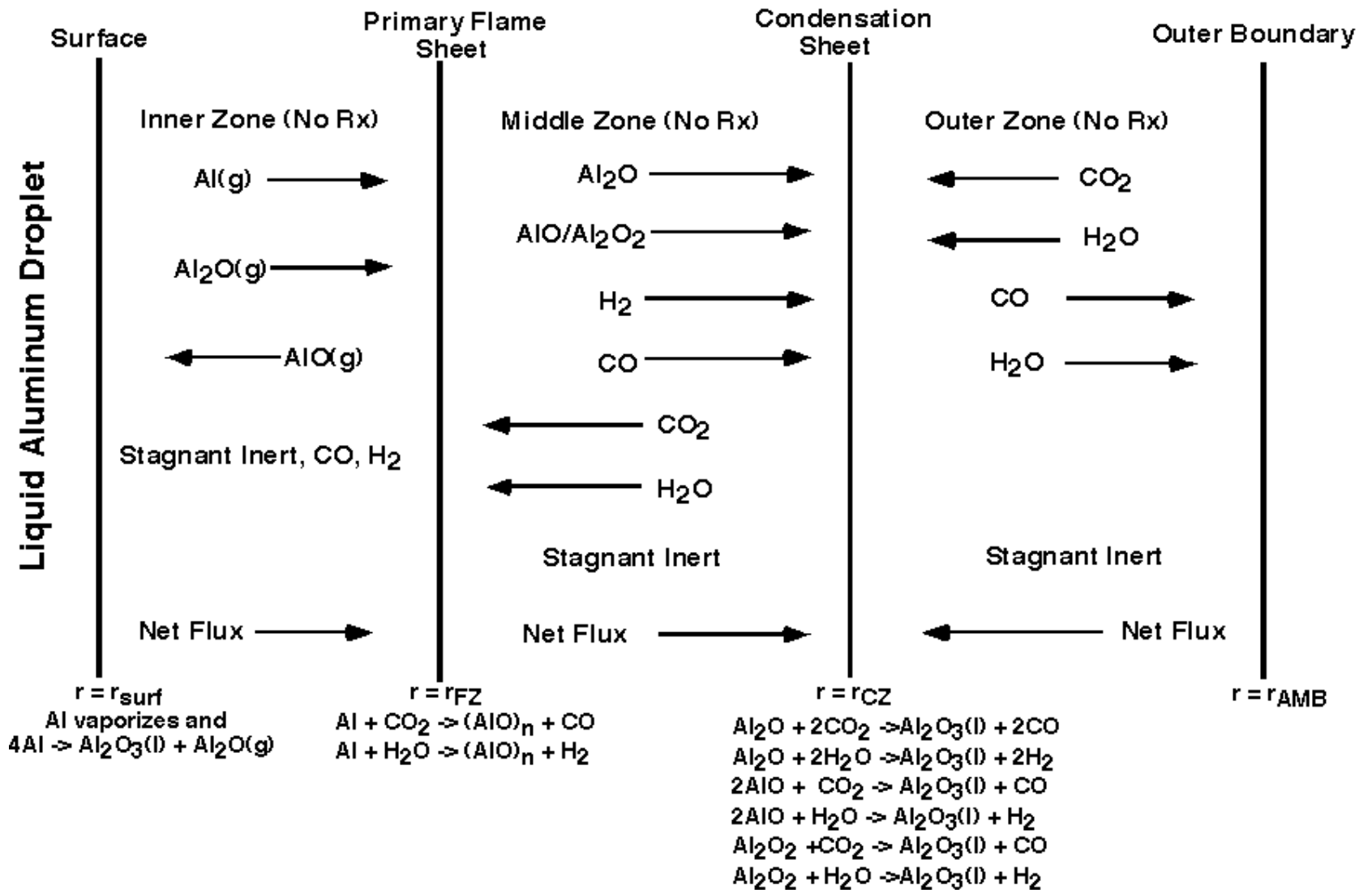


Figure 1. Sketch of Aluminum Combustion Model

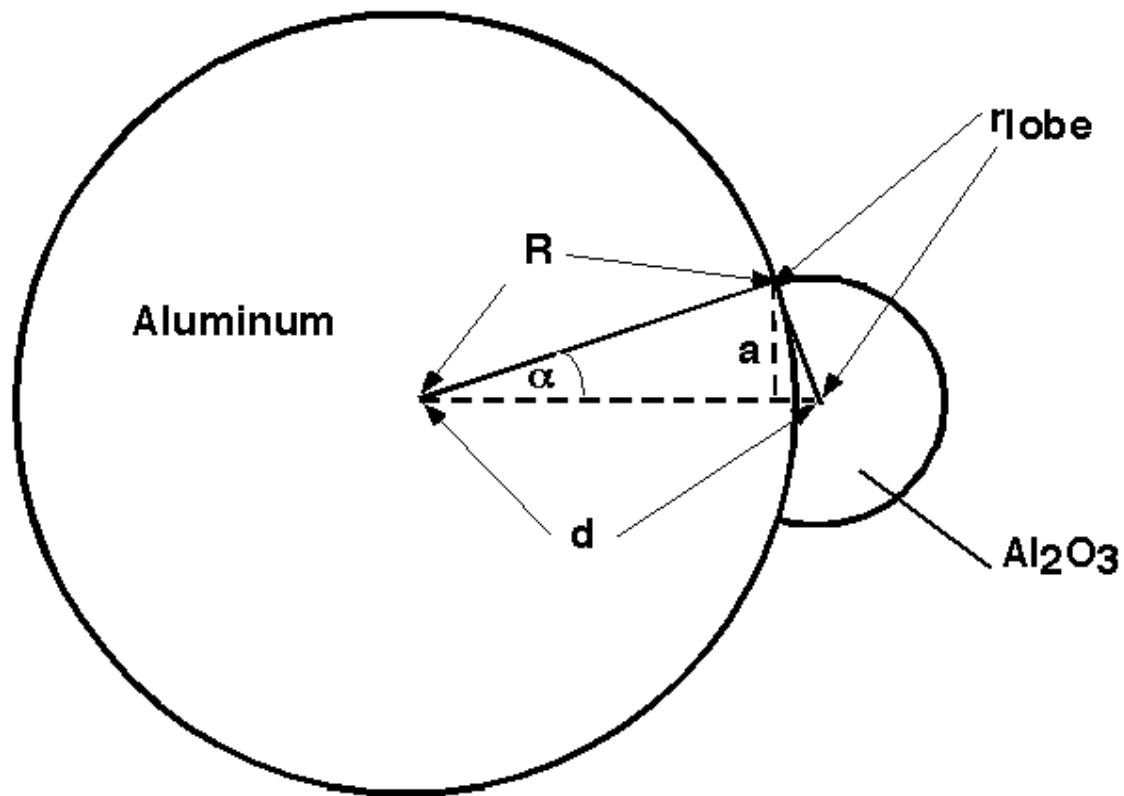


Figure 2. Sketch of Postulated Al- Al_2O_3 Lobe Geometry

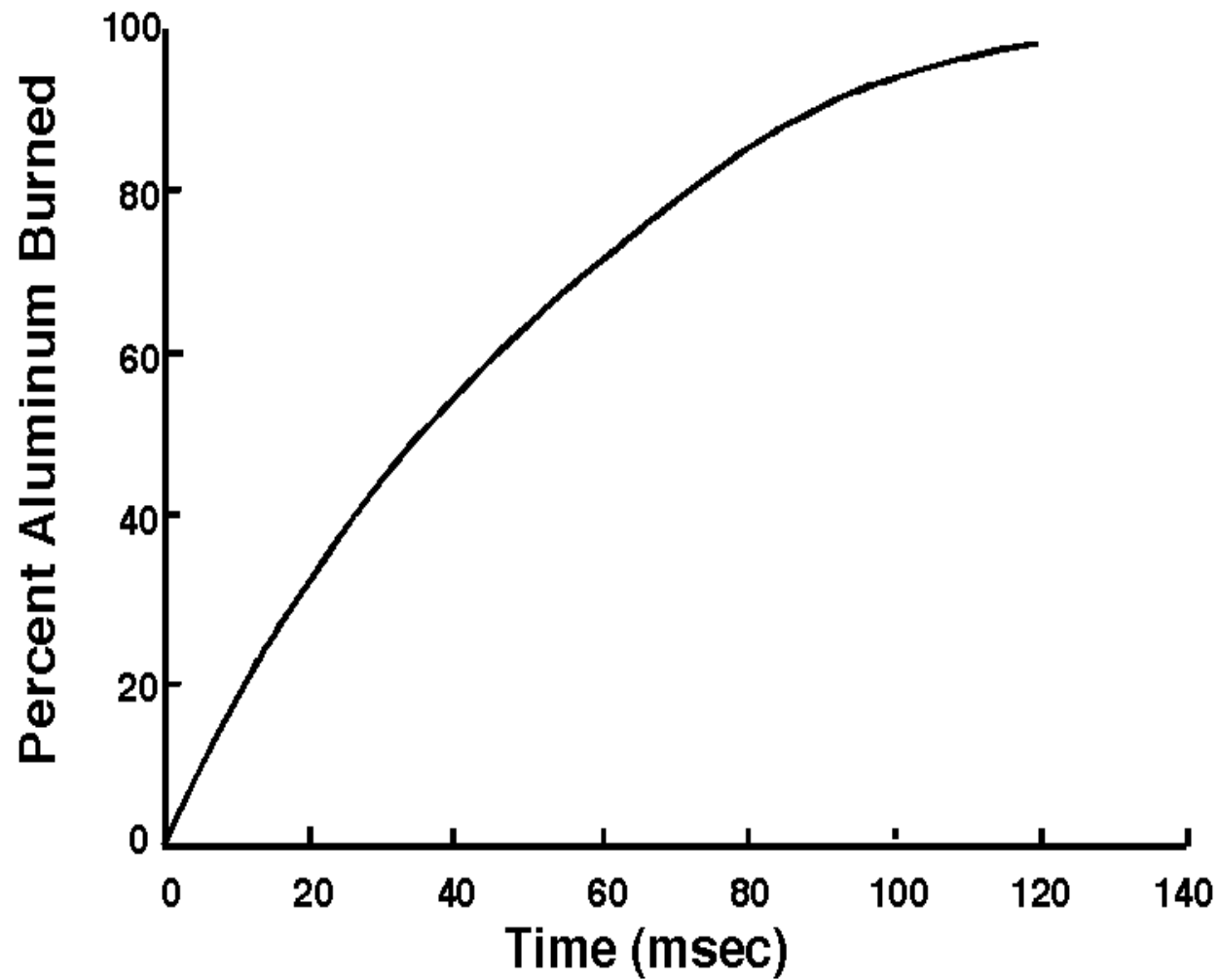


Figure 3. Percentage Aluminum Burned Versus Time

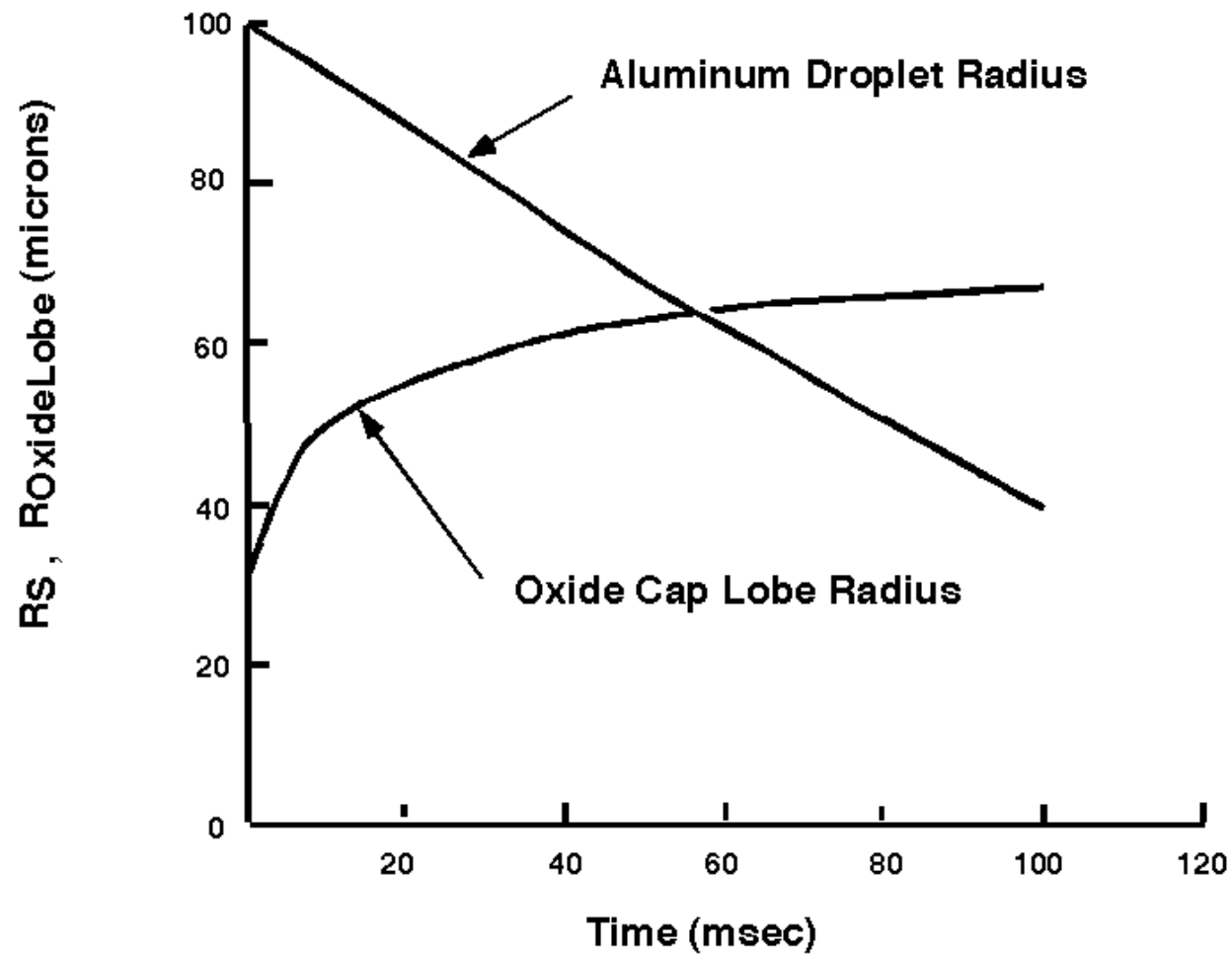


Figure 4. Radius of Al Sphere and Oxide Cap Lobe Vs Time

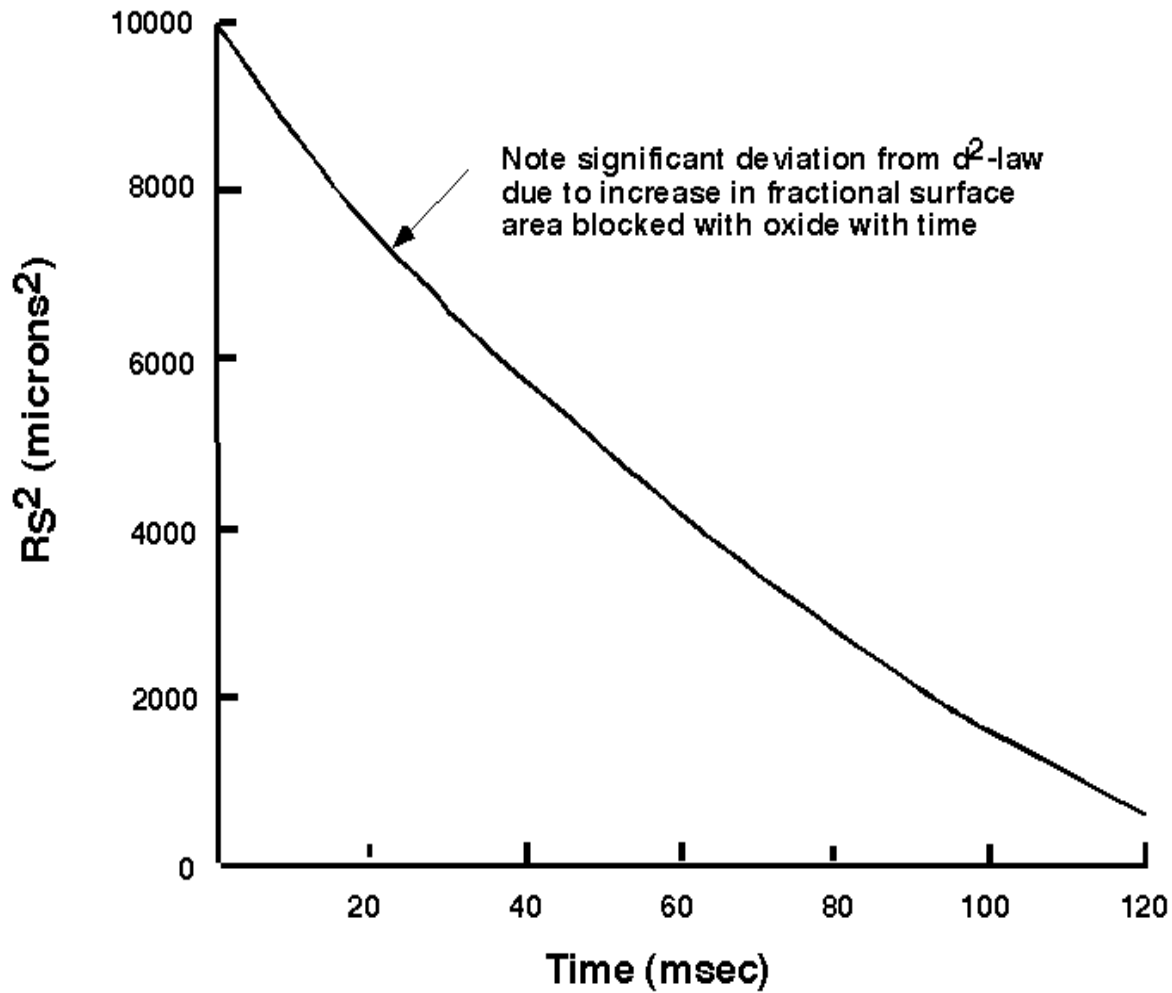


Figure 5. Square of Radius of Al Sphere Vs Time

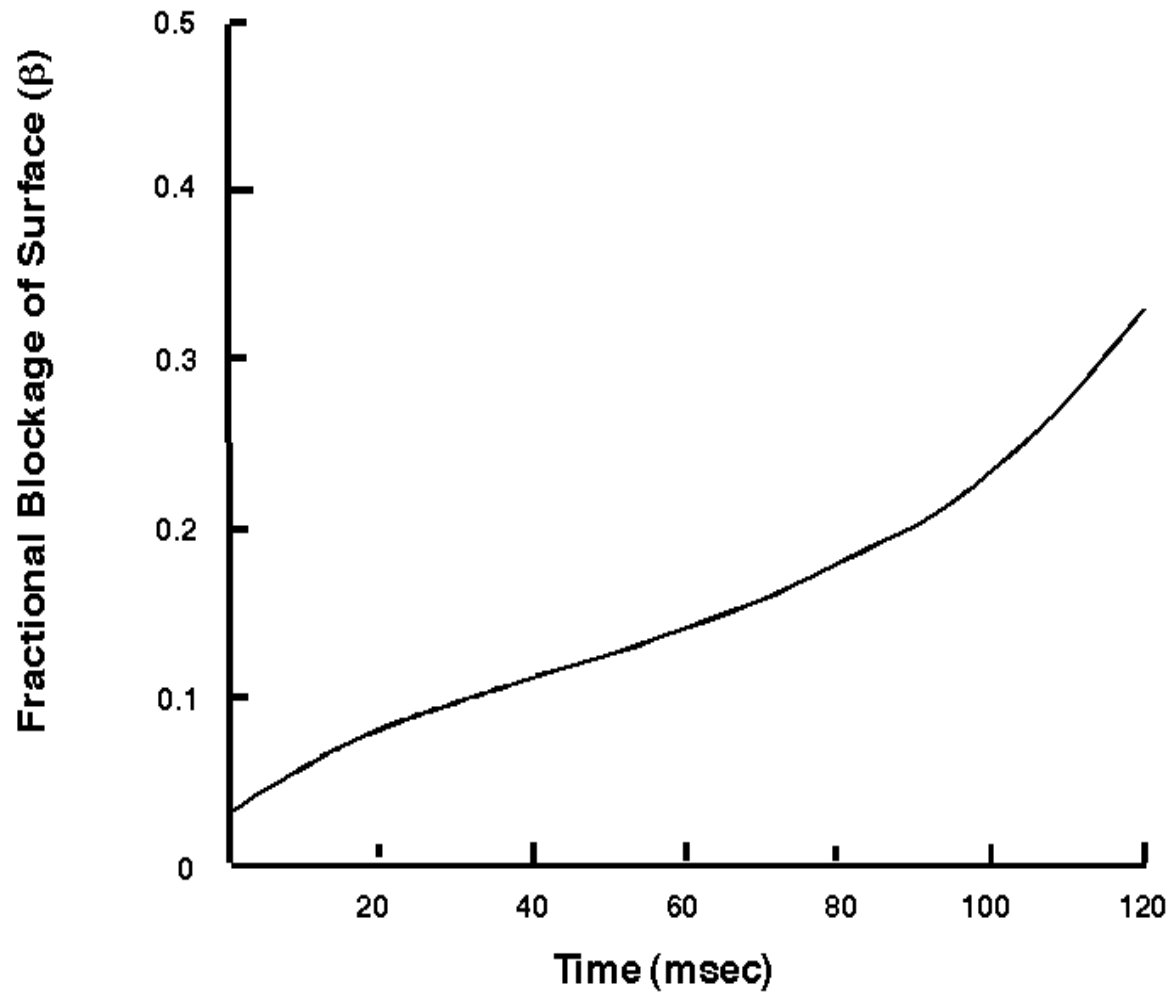


Figure 6. Fraction of Al Surface Area Blocked By Oxide Cap Vs Time

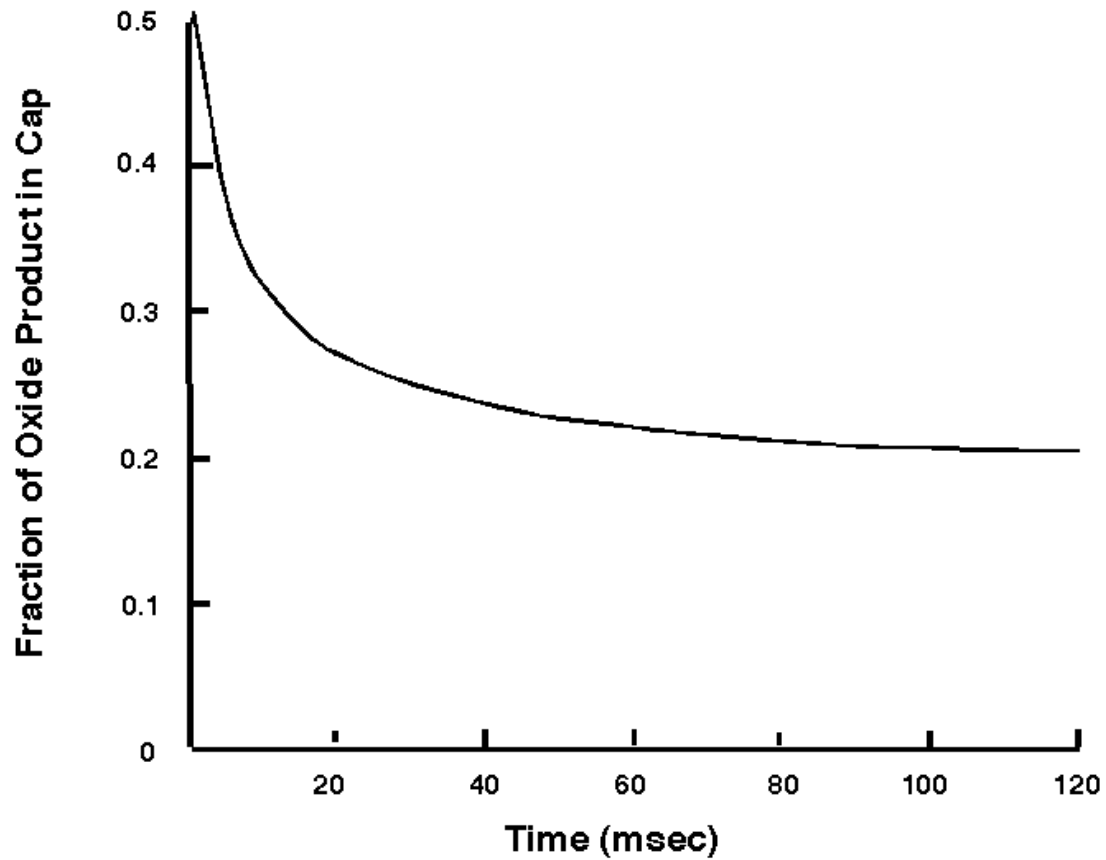


Figure 7. Percentage of Oxide Product Appearing in Cap Vs Time

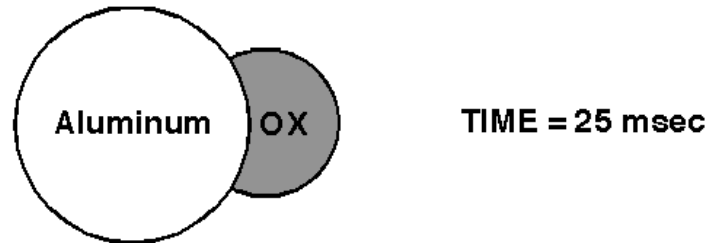
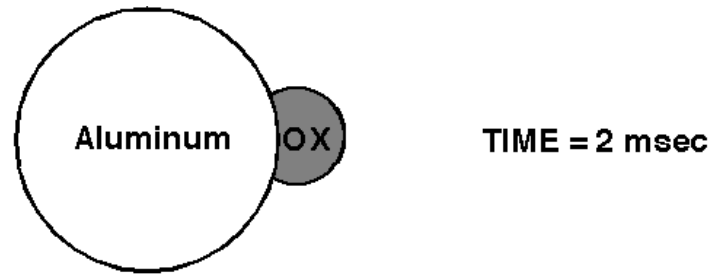


FIGURE 8. Evolution of Al-Al₂O₃ Shapes

Aluminum Combustion In a Solid Rocket Motor Environment

Merrill K. King
Consultant
Software & Engineering Associates, Inc
Carson City, NV
USA

August 0X, 2008

PRELIMINARY CALCULATIONS

- Aluminum vapor pressure versus temperature (chart on Slide 3)
- Estimation of burning aluminum surface temperature and mass fraction of Al adjacent to the surface using a very simplified B-Number analysis. Indicates surface temperature considerably below boiling point and surface mass fraction Al < 0.10.
- Calculation of pseudo-boiling point of Al_2O_3 . Ran several different types of thermochemistry calculations, concluding that the predominant Al_xO_y species will be Al_2O_3 liquid any place in the flame zone where the oxygen/aluminum atomic ratio is high enough to take it there.
- Examination of Babuk's claim that $4\text{Al}(\text{l}) + \text{Al}_2\text{O}_3(\text{l})$ will convert to $3\text{Al}_2\text{O}(\text{g})$ at the interface between Al and oxide in the cap region. Free energy calculations indicate that this will not occur at reasonable values of the surface temperature.

PRELIMINARY CALCULATIONS

- Definition of the most probable reaction(s) at the aluminum particle surface. A series of thermochemistry calculations at specified temperatures for various ratios of aluminum, oxygen, and argon mixtures indicate that at the surface these reactions will be aluminum vaporization and $4\text{AlO} \rightarrow \text{Al}_2\text{O}_3(\text{l}) + \text{Al}_2\text{O}(\text{g})$
- Additional free energy calculations indicated that for an environment where the principal oxidizers are CO_2 and H_2O , the likely sequence of reactions involves $\text{Al}(\text{g}) + \text{CO}_2 \rightarrow \text{AlO} + 1/2\text{Al}_2\text{O}_2 + \text{CO}$ and $\text{Al}(\text{g}) + \text{H}_2\text{O} \rightarrow \text{AlO} + 1/2\text{Al}_2\text{O}_2 + \text{H}_2$ at a primary flame sheet followed by further oxidation of $\text{Al}_2\text{O} + \text{AlO} + 1/2\text{Al}_2\text{O}_2$ with CO_2 or H_2O to produce $\text{Al}_2\text{O}_3(\text{l}) + \text{CO}$ and H_2 at an outer condensation sheet.
- Examination of the fraction of Al_xO_x which will appear as monomer versus dimer as a function of flame sheet temperature (little effect on species transport but a significant effect on flame temperature). Results of these calculations are shown in Slide 4 and built into the aluminum combustion code described later.

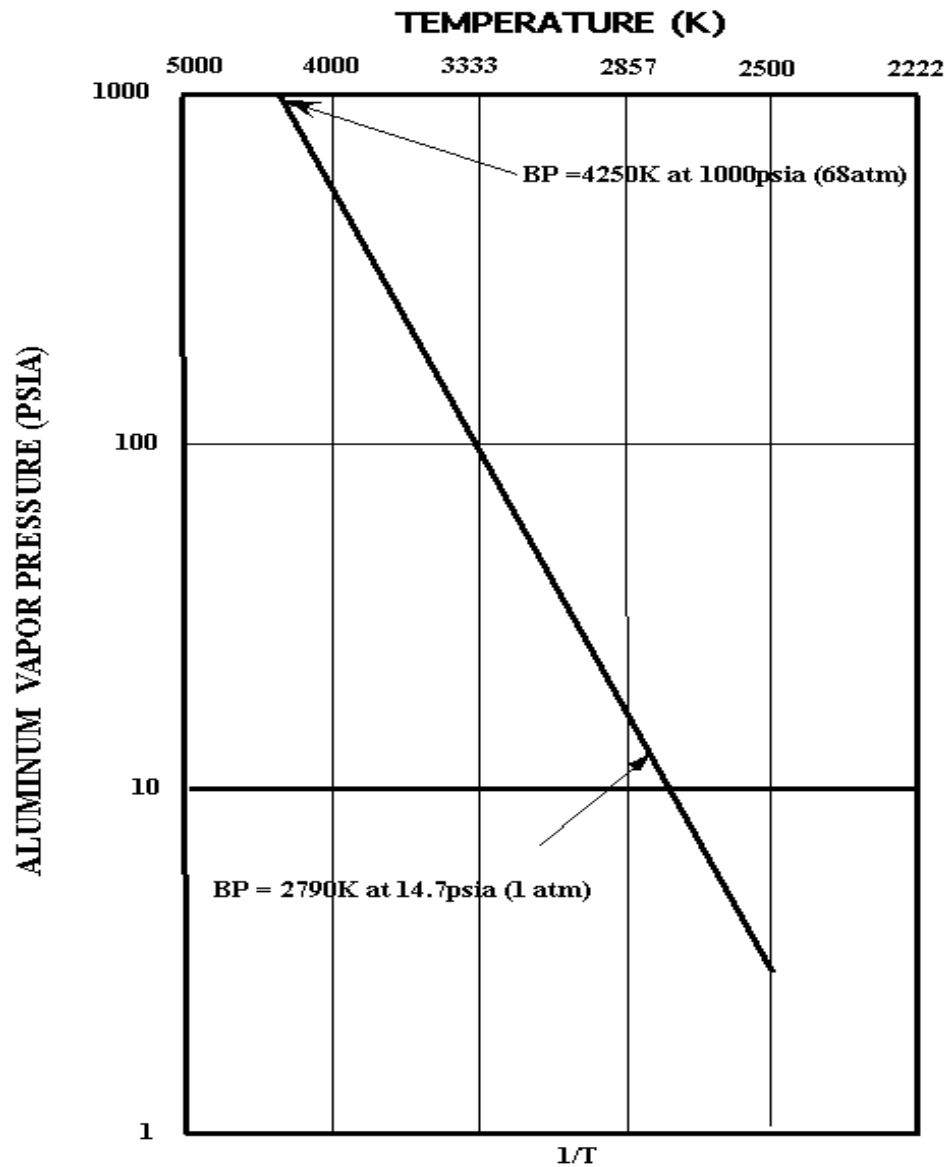


FIGURE 1. ALUMINUM VAPOR PRESSURE CURVE

Distribution A: Public Release; distribution unlimited

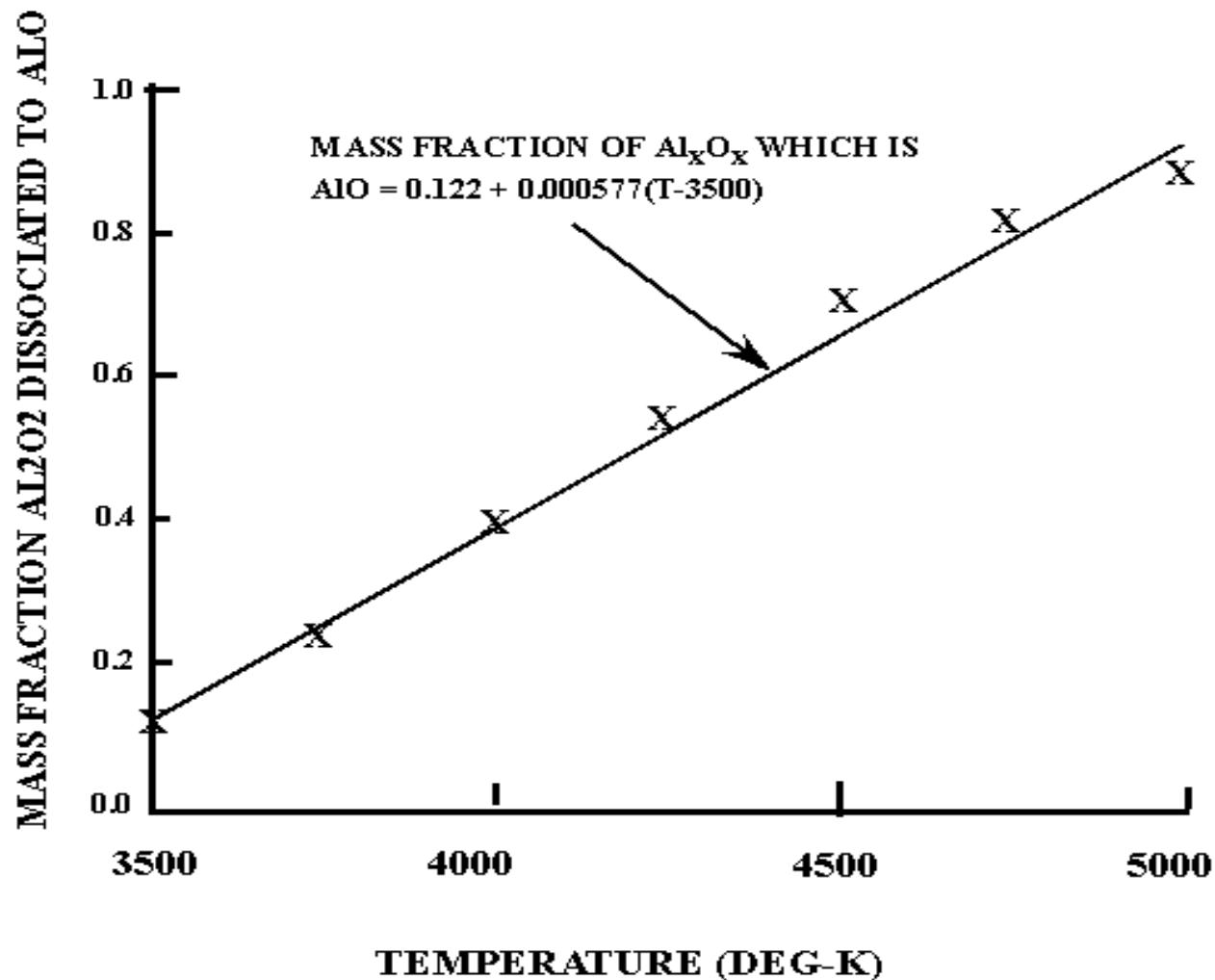
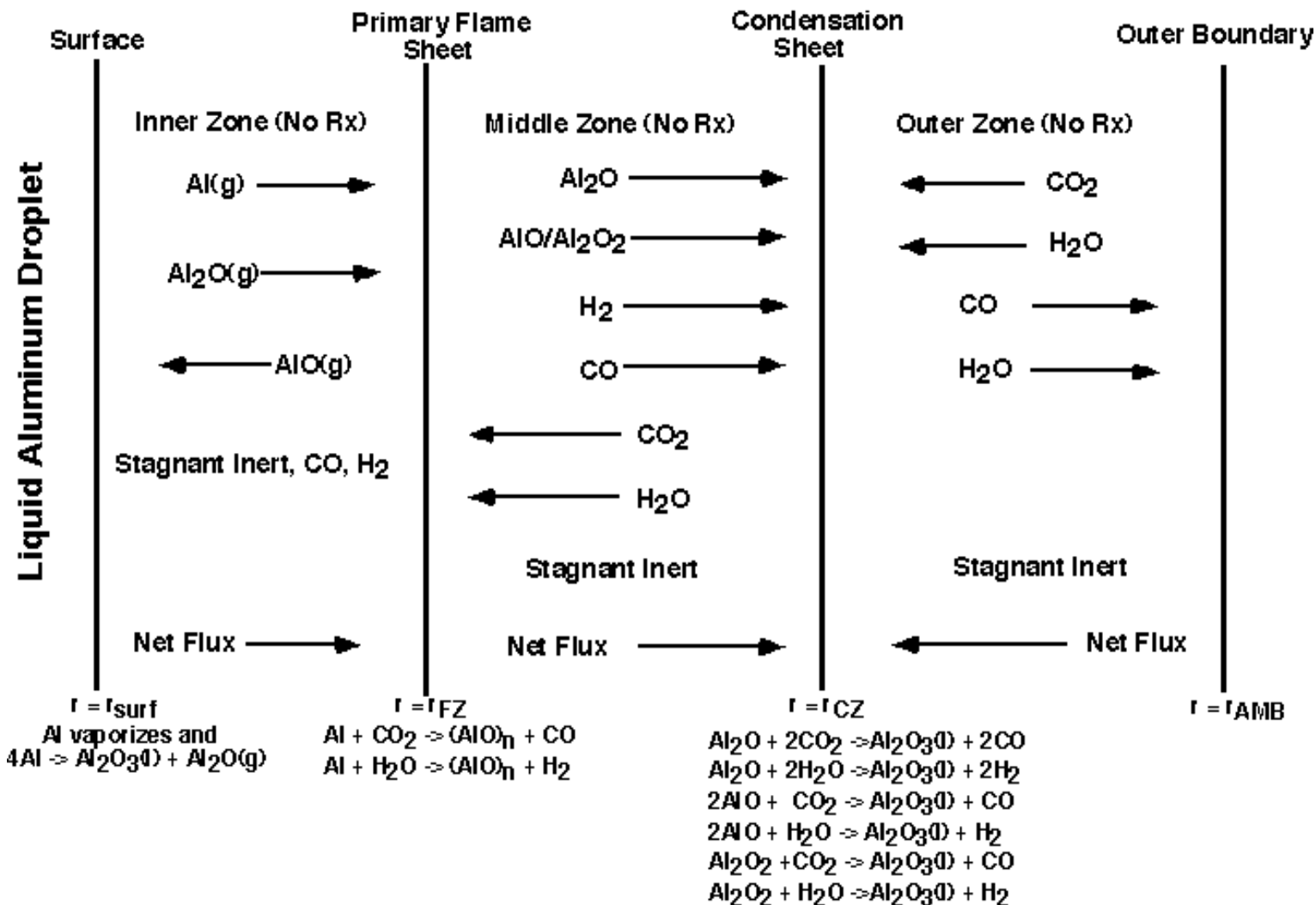


FIGURE 2. $AlO-Al_2O_2$ SPLIT VS FLAME ZONE TEMPERATURE

MAJOR ASSUMPTIONS AND APPROXIMATIONS

- Infinitesimally thin reaction sheets (infinitely fast reactions) at primary flame sheet and condensation sheet. AIO reaction rate at surface equal to collision rate multiplied by input collision efficiency
- Quasi-steady-state
- Fick's Law applies, with all Lewis Numbers = 1
- Constant ρ , D , c_p , MW_{MIX} , etc. across each zone, evaluated at midpoint T
- No gas-phase reactions in zones between the sheets: permits analytical integration of flux equations to algebraic forms
- Al_2O does not oxidize further at flame sheet, but reacts at condensation sheet
- Magical "sink" region at condensation zone for aluminum oxide smoke
- AIO monomer/dimer split determined by temperature at the flame sheet
- No radiative heat transfer
- Input value for T at the condensation sheet--fortunately weak dependence



GENERAL OUTLINE OF SOLUTION PROCEDURE

- End up with 42 equations in 42 unknowns: m_j 's, m_{Net} 's, and enthalpy fluxes across each zone, Y_j 's at surface, primary flame sheet, and condensation sheet, surface T, primary flame sheet temperature, radial locations of the primary flame sheet and the condensation sheet, rate of changes in aluminum mass and oxide cap mass, and rate of production of oxide smoke
- For given instantaneous ambient conditions, particle size, and oxide cap size, guess the rate of consumption of the aluminum droplet and accumulation of the oxide cap, and use a double-nested trial-and-error approach to home in the correct values
- Update property values as part of each loop

WRAP-AROUND STREAM-TUBE TRACKING CODE

- Next, the code described on the previous charts was imbedded as a called subroutine in a “wrap-around code” which keeps track of the “heating and eating” of the environment (increased ambient temperature due to heat released by the Al combustion and decreased oxidizer level due to CO₂ and H₂O consumption in the combustion).
- First, external calculations of temperature and composition of the stream-tube as a function of the percent aluminum burned for the given propellant formulation and pressure are made, and curve fits of temperature, mass fraction CO₂, mass fraction H₂O, etc as functions of the percent aluminum burned are developed and built into the “wrap-around code” which keeps track of progress of all variables along the stream-tube. In addition, curve-fits of aluminum and aluminum oxide densities vs temperature are built into this code.
- Also included in the “wrap-around code” is an algorithm for calculation of the changing geometry of the aluminum and its oxide cap as mass is removed from the aluminum and oxide cap mass increases with travel along the stream-tube. This algorithm permits updating of the fractional aluminum surface area coated by the cap (β) as Al combustion progresses. This algorithm involves assumption that the Al droplet is spherical and that the oxide lobe is a sector of a sphere which intersects the Al surface at a 90 degree angle as depicted in the next chart (possibly an oversimplification which will have to later be modified).

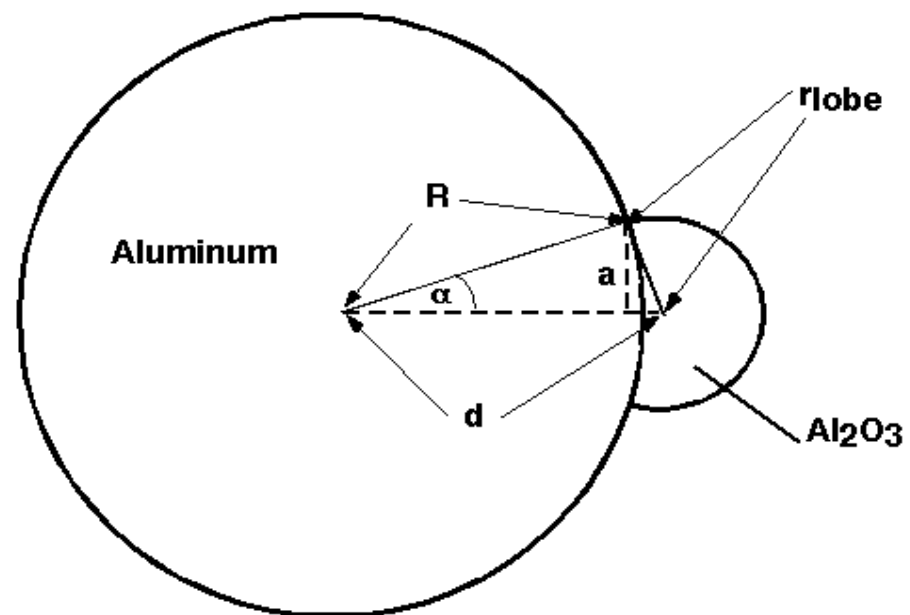


Figure 4. Sketch of Postulated Al-Al₂O₃ Lobe Geometry

SAMPLE PROBLEM DEFINITION AND OUTPUT

- The sample problem analyzed entails a 70/18/12 AP/Al/HTPB propellant burning at 68 atm (1000 psia)
- The chosen aluminum particle radius was 100 microns
- An initial uniform oxide coating thickness of 1 micron was selected, with assumption that it is drawn up into a cap at the time of ignition
- The input oxide smoke condensation temperature was chosen to be 4000 degrees-K
- It was also assumed that every collision of AlO with the aluminum surface results in reaction
- The input effective film radius around each particle was based on the aluminum particle spacing in the flow through the rocket motor, approximately 10 times the initial particle radius for this case
- Results are presented on the remaining charts

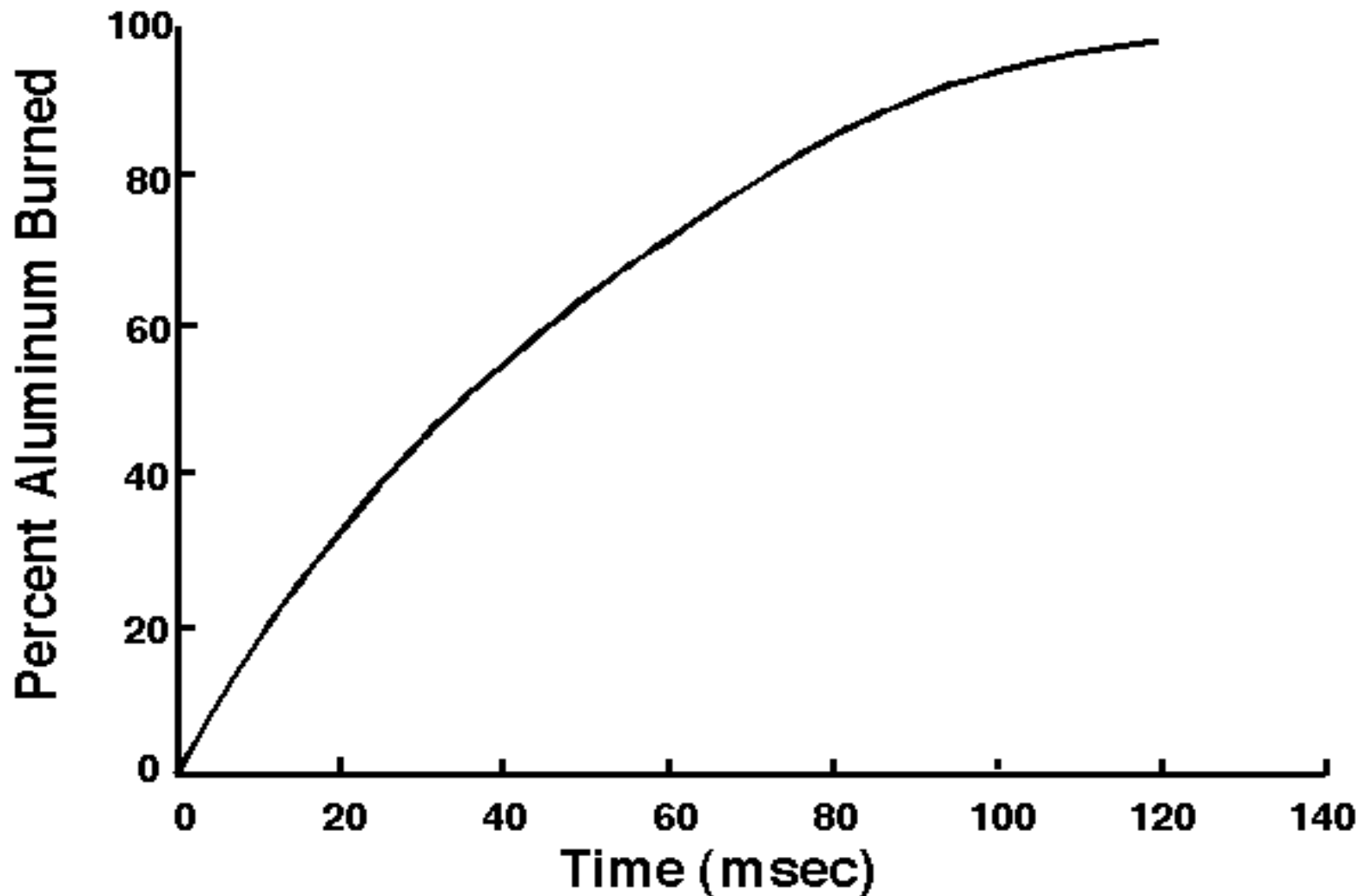


Figure 5. Percentage Aluminum Burned Versus Time

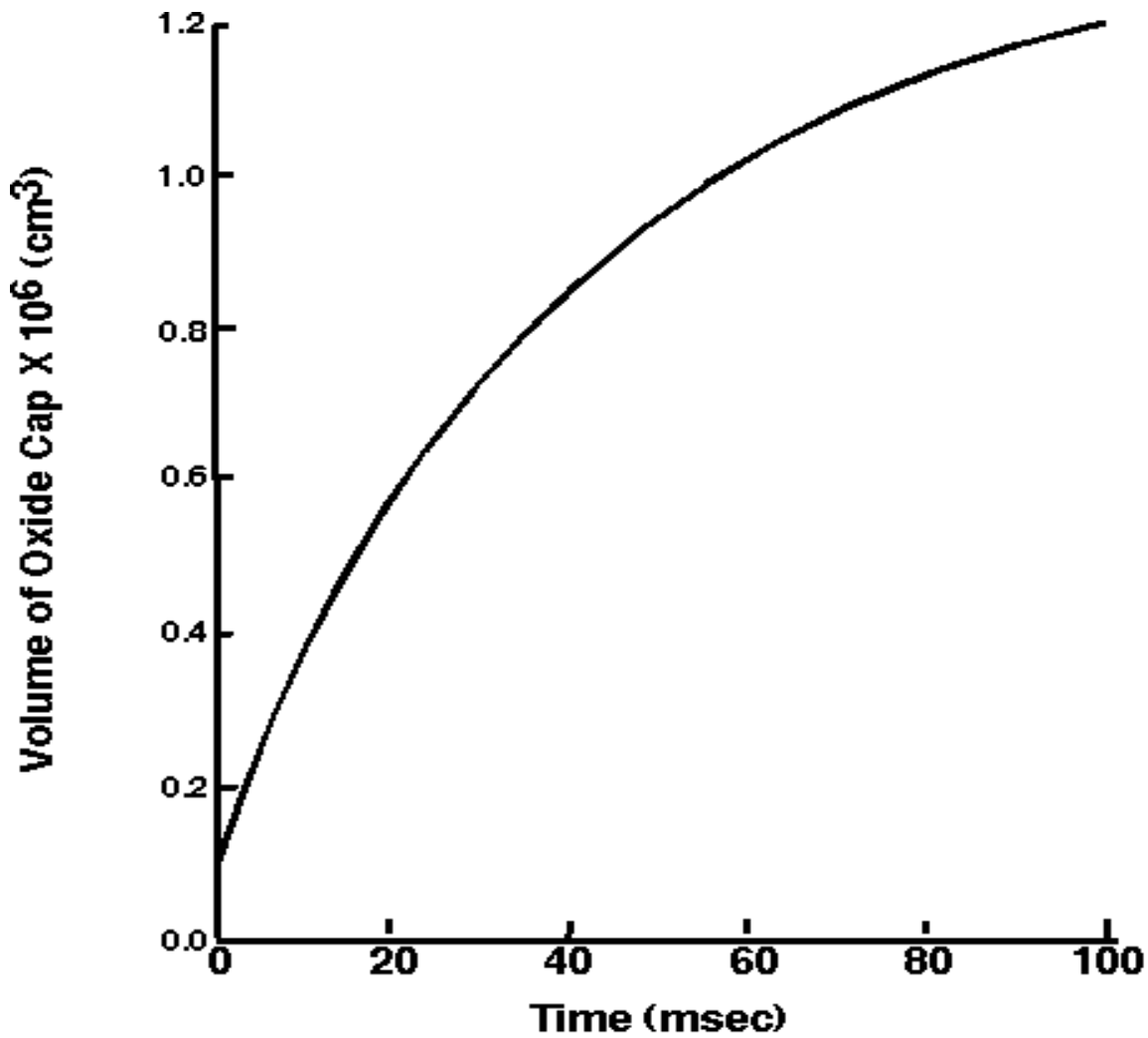


Figure 6. Volume of Oxide Cap Versus Time

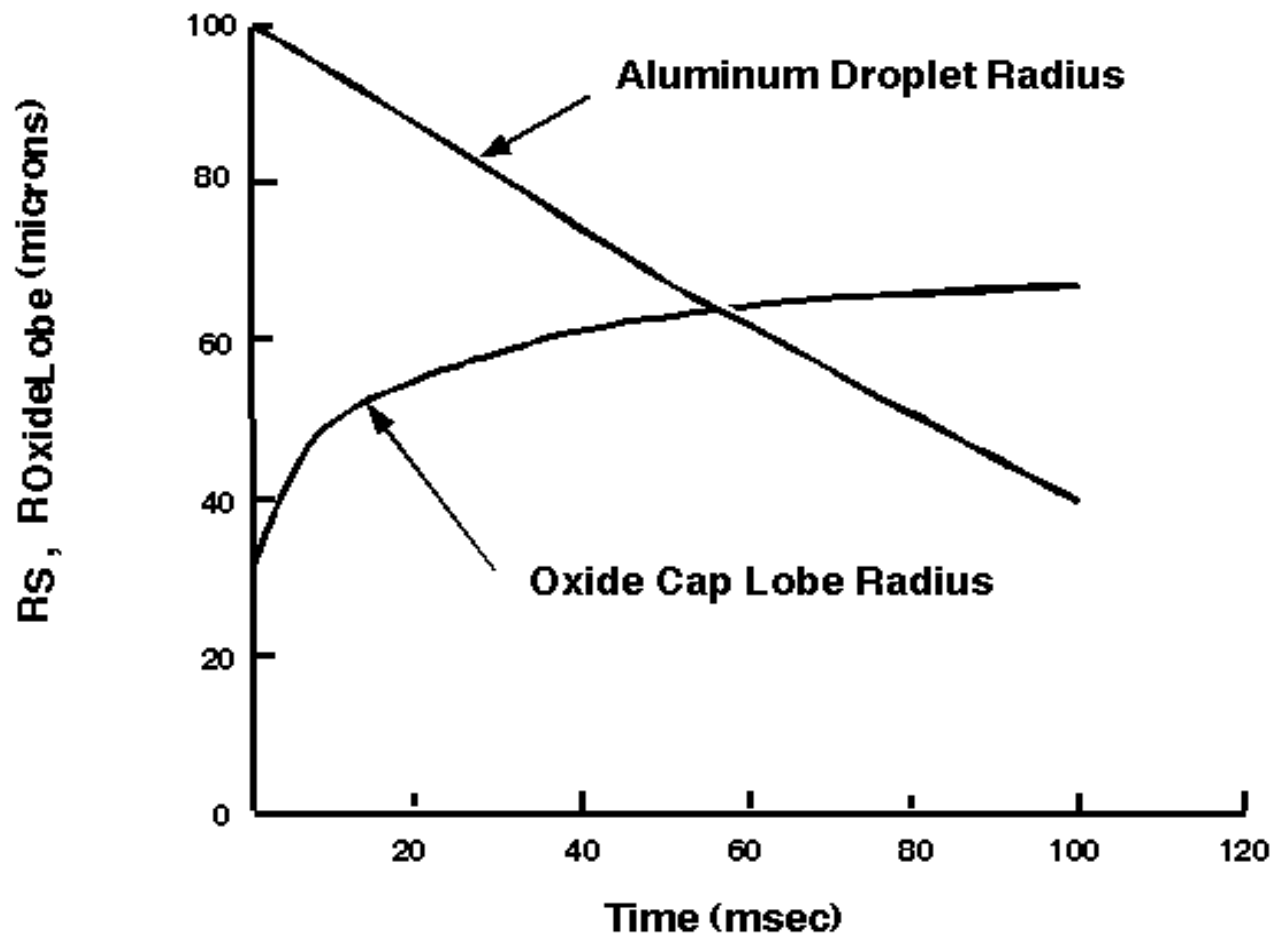


Figure 7. Radius of Al Sphere and Oxide Cap Lobe Vs Time

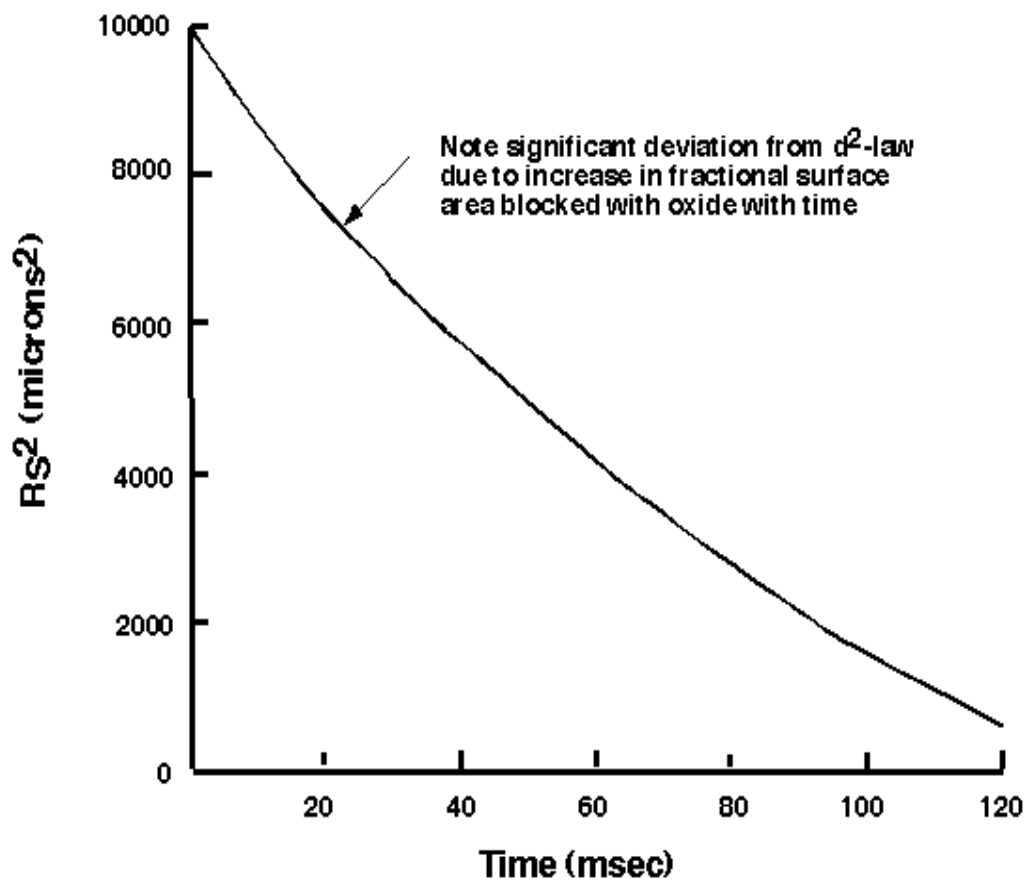


Figure 8. Square of Radius of Al Sphere Vs Time

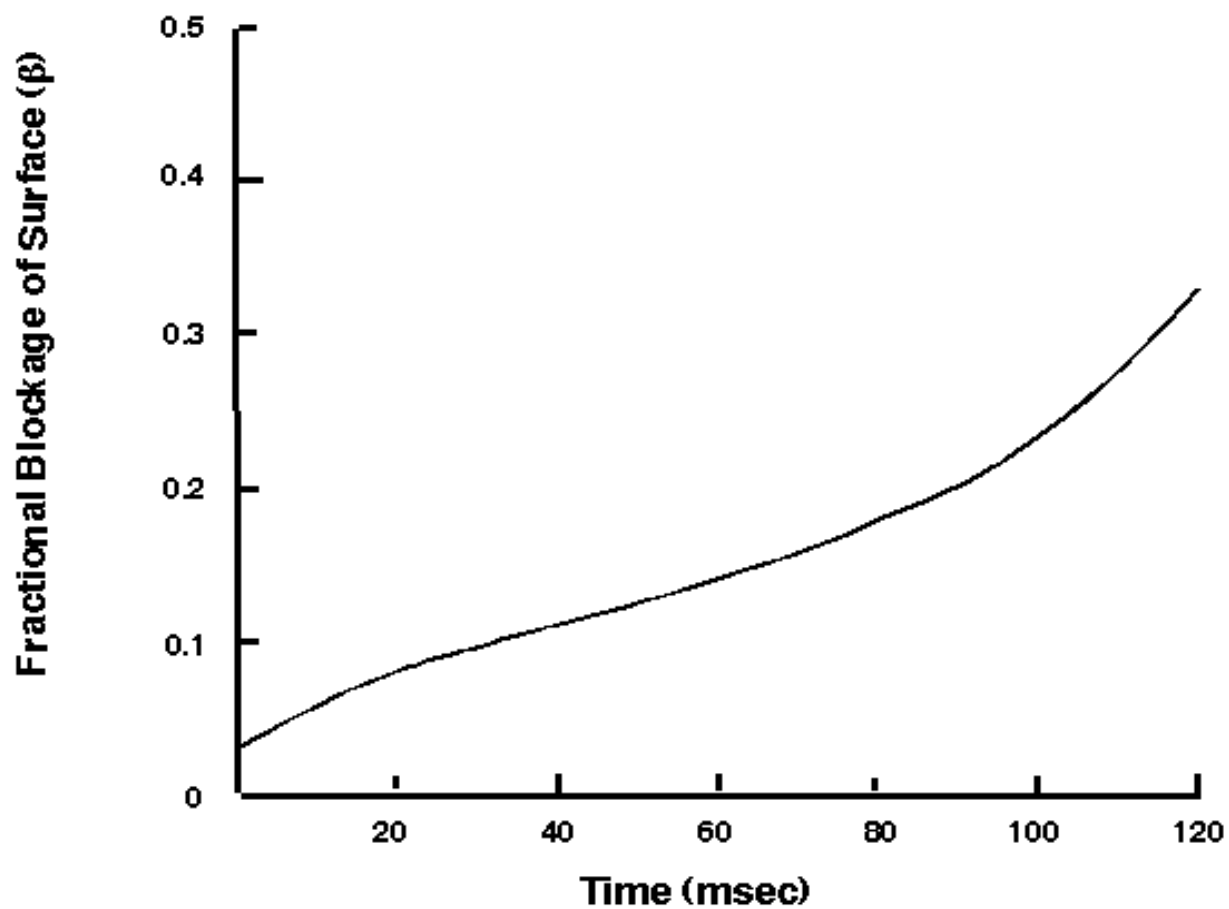


Figure 9. Fraction of Al Surface Area Blocked By Oxide Cap Vs Time

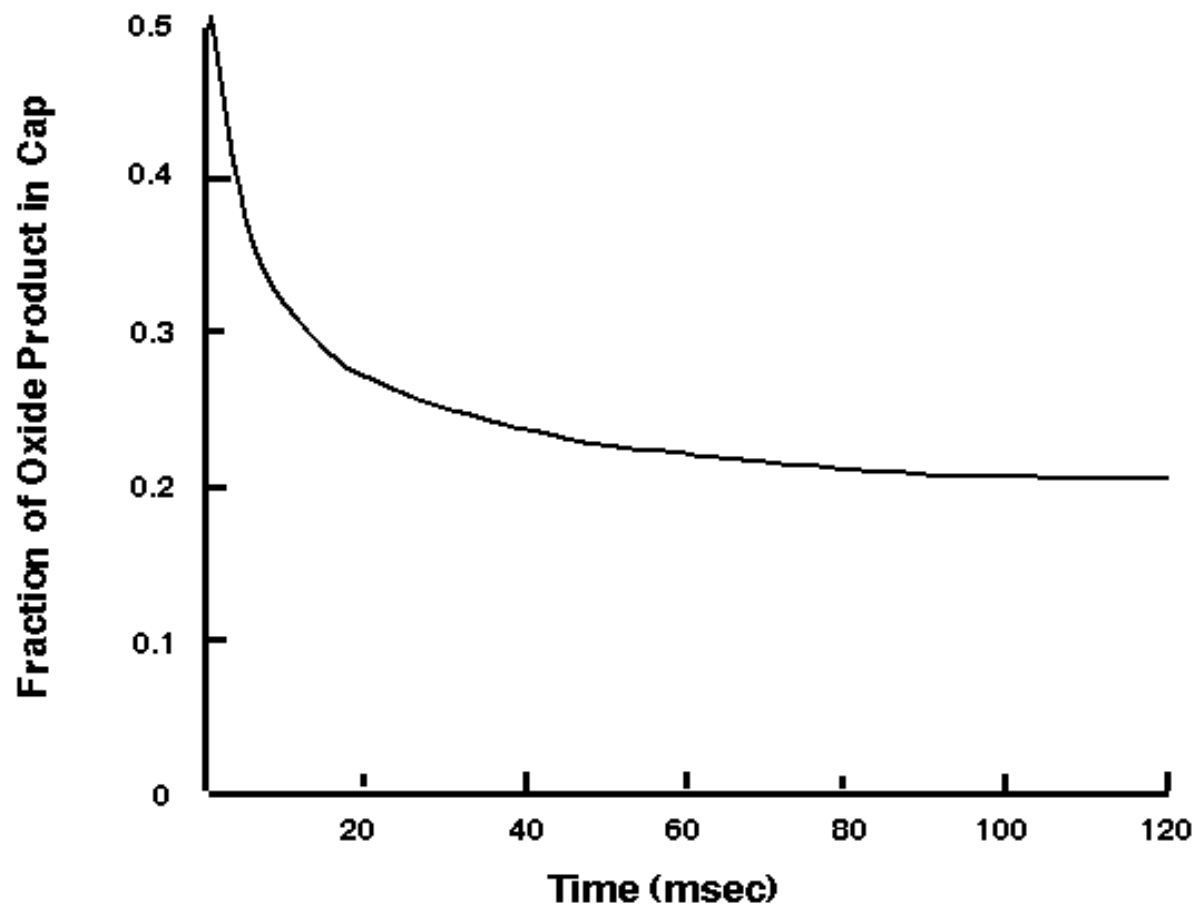


Figure 10. Percentage of Oxide Product Appearing in Cap Vs Time

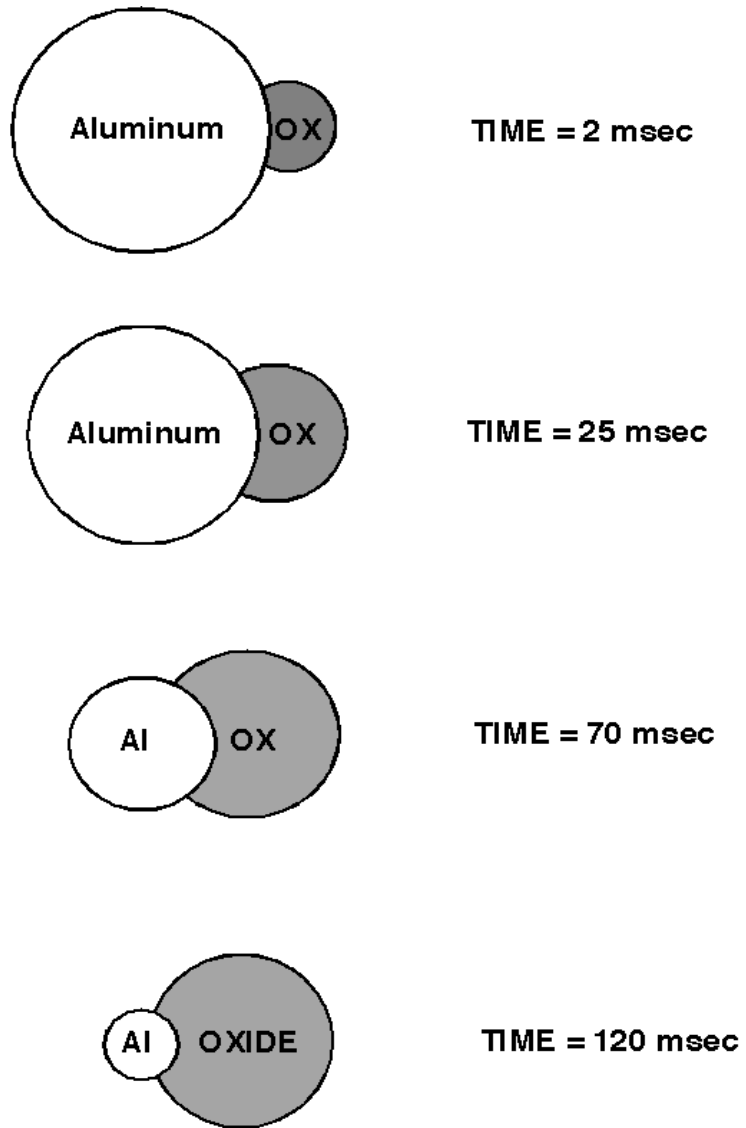


FIGURE 11. Evolution of Al-Al₂O₃ Shapes